JOURNAL OF MATERIALS SCIENCE 28 (1993) 5603–5609

The Bi–Sr–Ca–Cu–(Al)–O system; accompanying phases I

J. HYBLER, M. ŠIMEČKOVÁ, S. DURČOK
Institute of Physics, Czech Republic Academy of Sciences, Cukrovarnická 10, 16200 Praha 6, Czech Republic
F. VESELOVSKÝ
Geological Survey, Malostranské náměstí 19, 11821 Praha 1. Czech Republic

Bulk samples of superconductive cuprates BiSrCaCuO were prepared by melting of mixtures of oxides and carbonates, in alumina crucibles, using various thermal treatments. In some samples, several accompanying non-superconductive phases appeared. The later were studied by visual examination under the optical microscope, scanning electron microscopy, electron microprobe analysis and X-ray diffraction (single crystal precession and powder Gandolfi camera). Besides $Bi_2Sr_2CaCu_2O_8$ (further 2212) and $Bi_2Sr_2CuO_6$ (2201) BiSrCaCuO phases, CuO and Ca_2CuO_3 (with Sr content), another phase with composition $Bi_4Sr_{1.45}Ca_{2.31}Cu_{0.37}O_{10.13}$ was found in one sample in the form of oriented intergrowths with Cu_2O. The powder diffraction data enabled us to interpret the former compound as Bi_2SrCaO_5 with some Sr replaced by Ca. In addition, a yellow-coloured phase of approximate composition $BiSr_2CaAl_3O_9$, cubic, *F*-centred, (for two specimens $a = 2.486(6)$ nm or $a = 2.496(8)$ nm, was found in three samples heated to over 1040 °C. This phase resulted from the reaction with the alumina crucible. The X-ray precession and powder data are reported.

1. Introduction

About 30 bulk samples of BiSrCaCuO were prepared by melting in alumina crucibles each with various thermal histories. The detailed study of the first six samples showed that, besides the superconductive cuprates, other phases may also appear.

The most comprehensive list of binary and ternary phases from systems $SrO–\frac{1}{2}Bi_2O_3$, $CaO–\frac{1}{2}Bi_2O_3$, SrO–CuO, CaO–CuO, $SrO–CaO–\frac{1}{2}Bi_2O_3$ has been reported by Roth *et al.* [1]. The binary systems SrO–CuO, CaO–CuO were studied earlier by Teske and Müller-Buschbaum [2–5]. One of their phases was prepared by us, too. Conflant *et al.* [6] reported the phase diagram of the $CaO–Bi_2O_3$ binary and Guillermo *et al.* [7] of the $SrO–Bi_2O_3$ binary. A revision of the latter diagram and of SrO–CuO has been reported by Hwang *et al.* [8]. A description of all possible binary, ternary and quaternary systems is also in the paper of Hong *et al.* [9].

Our study has revealed the possibility of complicated intergrowths of additional phases. In addition, unwanted reaction of the alumina crucible with its contents is also possible at higher temperatures, so that some phases may contain aluminum as well. This work provides a description of accompanying phases identified and characterized up to now. The more detailed characteristics of superconductive cuprates from these samples are or will be described elsewhere. [10]

2. Experimental

2.1. Preparation of samples

All samples were prepared from melts with various starting compositions of Bi_2O_3, $SrCO_3$, $CaCO_3$, CuO and, in one instance, a minute amount of PbO. The atomic proportions of six samples relevant to this work are listed in Table I. All of them were prepared in alumina crucibles with the following thermal histories.

Sample Bi-6: heated in air to 1100 °C at an approximate rate of 200 °C h^{-1} then furnace cooled to 900 °C at an approximate rate of 100 °C h^{-1}, reheated for 8 h to 980 °C, cooled to 900 °C (~ 100 °C h^{-1}), twice heated to 960 °C (~ 200 °C h^{-1}) and cooled to 880 °C (~ 100 °C h^{-1}), twice heated to 960 °C (~ 200 °C h^{-1}) and cooled to 860 °C (~ 100 °C h^{-1}), then cooled at a rate of 10 °C h^{-1} to 640 °C and finally furnace cooled to room temperature.

Sample Bi-9: Heated in air to 1014 °C (~ 200 °C h^{-1}), cooled in 4 h to 874 °C, then cooled at

TABLE I Starting compositions of samples; atomic proportions

Sample	Bi	Sr	Ca	Cu	Pb
Bi-6	2.0	1.5	1.5	1.0	
Bi-9	1.6	1.0	1.0	1.6	
Bi-12	2.3	1.0	1.0	2.3	
Bi-18	1.6	1.0	1.0	1.6	
Bi-22	1.5	1.0	1.0	1.6	0.1
Bi-26	1.6	1.0	1.0	1.6	

0022–2461

a rate of 2 °C h^{-1} to 782 °C and finally 1 day furnace cooled to room temperature.

Sample Bi-12: heated in air to 1050 °C (~ 200 °C h^{-1}), then soaked for 5 h, heated to 1097 °C(~ 200 °C h^{-1}), soaked for 10 h, cooled (3 °C h^{-1}) to 956 °C, cooled in 27 h to 834 °C, cooled (10 °C h^{-1}) to 760 °C and then 1 day furnace cooled as above.

Sample Bi-18: heated in oxygen for 15 h to 1000 °C, then cooled for 10 h to 900 °C, cooled for 60 h to 751 °C and finally for 70 h to room temperature.

Sample Bi-22: heated in oxygen over a period of 2 days to 1040 °C, cooled in air to 1018 °C (~ 100 °C h^{-1}), then to 833 °C (1.5 °C h^{-1}), and finally furnace cooled (~ 100 °C h^{-1}) to the room temperature.

Sample Bi-26: heated in air to 1000 °C (~ 200 °C h^{-1}), cooled for 22 h to 865 °C and finally furnace cooled (~ 100 °C h^{-1}).

2.2. Preliminary check and studies

Fragments of the bulk samples were first checked under a stereomicroscope. Usually they contained aggregates of plate-like crystals of superconductive cuprates of about 0.5–2 mm wide and 0.02–0.2 mm thick along with intergrowths of other accompanying phases. Sometimes, large tabular crystals of the BiSrCaCuO 2212 phase, CuO or needle-like crystals of Ca_2CuO_3 appeared on the surface or in the cavities. Some of these crystals were carefully removed for other studies. Part of the remainder of the sample was crushed and individual homogeneous appearing crystals, typically a few tenths of a millimeter in size, were separated under the stereomicroscope. The transparent crystals were checked for optical anisotropy in polarized light. Some larger fragments of the bulk sample (not homogeneous) were mounted in epoxy resin and polished for the electron microprobe and scanning electron microscopy studies. These sections were first checked with an optical microscope and photographed (on color slides) before coating with carbon film.

2.3. Electron microprobe analysis (EMA) and scanning electron microscopy (SEM)

A Jeol Superprobe 733 electron microprobe was used to determine the chemical composition. A polished section was first checked by SEM and individual phases were found by comparison with colour slides of the same area previously made in the optical microscope. The overall chemical composition was usually first checked by energy-dispersive X-ray analysis (EDX). Then several point analyses were performed. Sometimes we had difficulties with an exact localization of individual phases on the polished sections. Therefore, some analyses were performed on the separated homogeneous appearing fragments instead of polished sections. As the standards, pure metals were used for Bi, Al and Cu, $SrTiO_3$ for Sr and $CaMgSi_2O_6$ (diopside) for Ca. The *K*-lines of Cu, Ca and Al, *L*-line of Sr and *M*-line of Bi were used. The accelerating voltage was 20 kV. The results of all analyses are listed in Table II. Since the composition for many of the compounds varied from point to point, the average values, e.s.d. values, minimum and maximum values are reported in these instances.

2.4. Powder X-ray diffraction

Since the typical amount of the phases separated from the sample was too minute to allow studies on a diffractometer, a 114.6 mm Gandolfi camera [11, 12] with unfiltered CoK_α radiation ($\lambda_{\bar{\alpha}}$ = 0.17902 nm), in a Straumanis setting, was used to obtain the powder diffraction pattern of several phases. For better randomization, a cluster of single crystals, instead of one crystal, was placed in the beam. Unfiltered radiation was used for higher intensity . However, each line had to be tested for the appearance of the corresponding β-line at the expected place and such β-lines were omitted. Practically, only a few of the most intense β-lines exceeded background. The X-ray tube had previously been tested for the presence of *WL* lines by obtaining diffractograms of known substances.

Bulk samples of the superconductive cuprates were studied by a standard powder diffractometer with Ni-filtered CuK_α radiation.

2.5. Single crystal X-Ray diffraction

Some selected crystals were mounted on a goniometric head and studied by precession and cone-axis methods. In all cases, Nb-filtered MoK_α radiation (λ = 0.07107 nm) was used. Front reflection Laüe patterns were, if necessary, also performed on the precession camera set on zero precession angle.

3. Results and discussion

3.1. Superconductive cuprates

X-ray powder diffraction studies of bulk samples were performed on a standard diffractometer. Special attention has been taken of 0 0 2 peaks in the low angle region. Their position enables quick identification of individual phases. According to Huang *et al.* [13], for CuK_α radiation, the position of this peak is at about 4.8° (2θ) for the 3.8 nm–1 1 0 K–2 2 2 3 phase and 5.8° (2θ) for the 3.0 nm–80 K–2 2 1 2 phase. Similarly, the peak value for the 2.4 nm–2 2 0 1 phase is at about 7.3° (2θ)

In our samples, the (0 0 2) peak of the 80 K–2 2 1 2 phase appeared in samples Bi-6, Bi-9, Bi-18 and Bi-22; the (0 0 2) peak of the 2.4 nm–2 2 0 1 phase was observed in Bi-6, Bi-9, Bi-12 and Bi-22. No (0 0 2) peak of the 3.8 nm–1 1 0 K–2 2 2 3 phase appeared in any of the samples mentioned in this paper.

Good quality plate-like single crystals of the 3.0 nm–80 K–2 2 1 2 phase were separated from samples Bi-6 and Bi-18 and studied by the precession method. Precession photographs confirmed the orthorhombic symmetry and modulation along the *b*-axis. The crystal data are in Table III, compared with those of Gao *et al.* [14].

TABLE II Results of the electron microprobe analysis (wt. % of oxides, at % of elements)

Phase	Sample		Bi_2O_3	SrO	CaO	CuO	Al_2O_3
CuO	Bi-6		0.2	0.6	0.0	99.2	0.0
	Bi-9		1.2	0.5	0.0	98.3	0.0
	Bi-12		0.2	0.3	0.0	99.5	0.0
		(per 1 analysis)					
Ca_2CuO_3	Bi-26						
	average		0.2	6.9	55.0	37.6	[a]
	e.s.d.		0.1	0.4	0.7	0.5	
	min.		0.0	6.5	54.0	37.4	
	max.		0.3	7.7	55.9	38.5	
	at % of elements		0.0	2.0	32.3	15.5	
		(6 analyses)					
"Red phase"—	Bi-6						
admixtures	average		1.3	2.6	0.4	95.6[b]	[a]
	e.s.d.		0.5	2.5	0.6	3.1[b]	
	min.		0.8	0.9	0.0	92.2[b]	
	max.		1.8	5.4	1.1	98.2[b]	
	at % of elements		1.3	1.2	0.3	64.2[b]	
		(3 analyses)					
"Red phase"—	Bi-6						
matrix	average		76.4	12.4	10.6	2.3	[a]
	e.s.d.		2.0	2.0	1.1	1.1	
	min.		73.8	9.9	9.5	0.4	
	max.		78.9	14.9	12.2	3.6	
	at % of elements		21.8	7.9	12.6	2.0	
		(7 analyses)					
"Yellow	Bi-6						
phase"	average		39.9	28.1	7.9	1.0	21.4
	e.s.d.		3.4	0.9	0.5	0.2	1.9
	min.		36.6	27.1	7.4	0.8	18.7
	max.		44.2	29.3	8.6	1.4	23.0
	at % of elements		7.3	11.7	6.1	0.6	18.0
		(4 analyses)					
	Bi-12						
	average		44.1	23.3	8.0	0.7	22.4
	e.s.d.		4.2	1.1	0.7	0.2	1.2
	min.		36.5	21.7	6.8	0.4	20.6
	max.		47.6	24.4	8.6	1.0	23.5
	at % of elements		8.1	9.6	6.2	0.5	18.8
		(5 analyses)					
	Bi-22						
	average		38.9	31.4	7.5	2.1	23.7
	e.s.d.		2.9	3.0	1.0	0.2	2.8
	min.		33.7	26.3	6.6	1.8	19.0
	max.		40.9	34.2	9.1	2.3	26.2
	at % of elements		6.5	12.0	5.3	1.1	18.5
		(5 analyses)					

[a] Not indicated in the preliminary EDX search.
[b] Cu_2O.

TABLE III The crystal data for the 2212 phase from samples Bi-6 and Bi-18; precession camera, Nb-filtered MoK_α radiation, λ = 0.07107 nm

Sample	*a*(nm)	*b*(nm)	*c*(nm)
Bi-6	0.539(2)	0.540(1)	3.072(15)
Bi-18	0.540(1)	0.540(1)	3.060(5)
Gao *et al.* [14]	0.5413(1)	0.5408(1)	3.0871(5)

Crystals are modulated along the *b* axis.

Preliminary microprobe analyses on polished sections of samples Bi-6, Bi-9, Bi-12 revealed compositions rather different from the ideal 2212 or 2201. In Bi-6, we found areas of approximate composition $Bi_2Sr_{1.4}Ca_{1.3}Cu_{2.1}O_{7.6}$ (Fig. 4, dark grey lamellae) and of $Bi_2Sr_1Ca_{0.3}Cu_1O_{5.4}$ (light grey lamellae or rims of dark grey ones). The former is close to 2212 with some Sr replaced by Ca, whereas the latter is rather Sr-deficient 2201 with some Ca. In Bi-9, the composition varied around $Bi_2Sr_{1.3}Ca_{1.2}Cu_{1.2}O_{6.7}$ and in Bi-12 around $Bi_2Sr_{0.5}Ca_{0.4}Cu_{0.8}O_{4.7}$.

3.2. CuO

The copper oxide appeared in samples Bi-6, Bi-9 and Bi-12, usually as inclusions of black hypidiomorphic crystals in the bulk mass, more rarely as tabular single crystals in the cavities. It is very difficult to distinguish them from BiSrCaCuO superconductive phases by optical means, because of their similarity in colour. Nevertheless, the mechanical properties are different; CuO crystals are fragile, whereas those of

"BiSrCaCuO" are soft and flexible. On the SEM images CuO is much darker (See Fig. 1). A $0.2 \times 0.25 \times 0.05$ mm tabular crystal of CuO was removed from sample Bi-12 and studied by the precession method. The crystal data, Table IV, are consistent with those of Asbrink and Norby [15]. The chemical analyses from three samples are given in Table II.

3.3. Ca_2CuO_3

This phase appeared in sample Bi-26 in the form of prismatic needle-like crystals elongated along *a*. A SEM photograph of typical crystals is given in Fig. 2. The unit cell parameters determined from the *hkO*, *hOl* and *Okl* precession photographs are given in Table V, and compared with those reported by Teske and Müller-Buschbaum for Ca_2CuO_3 [3] and Sr_2CuO_3 [2]. Although the unit cell parameters were not sensitive enough to indicate lattice expansion, the results of electron microprobe analysis (Table II) showed that part of the calcium is replaced by strontium. From Table II, the formula is $Sr_{0.12}Ca_{1.94}Cu_{0.94}O_3$.

3.4. "Red phase"

The space between the tabular crystals of "BiSrCaCuO" in sample Bi-6 is filled by a remarkable red material. The separated fragments are light red, translucent on the margins. The SEM studies of polished sections reveal that this material is not a single phase but consists of rod-like (or channel-like), parallel oriented, perhaps epitaxial admixtures (precipitates?) of one phase (darker in the SEM) in a light matrix. (Figs 3–5) These rods are nearly parallel in some regions. Their form, which varies from dots through ovals to thick lines, can be seen in cross-sections of variously oriented regions (see Fig. 5). The results of

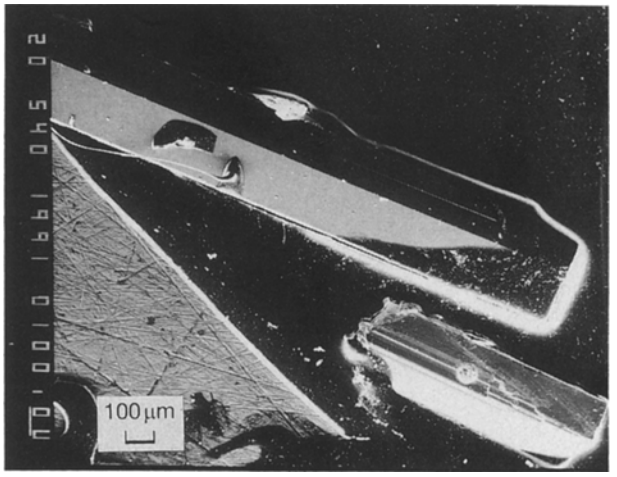

Figure 2 The SEM image of prismatic crystals of Ca_2CuO_3 isolated from sample Bi-26.

TABLE V The crystal data for Ca_2CuO_3 from sample Bi-26; precession camera, Nb-filtered MoK_α radiation, $\lambda = 0.07107$ nm

	a(nm)	*b*(nm)	*c*(nm)
Ca_2CuO_3 (this work)	0.378(1)	1.223(3)	0.326(1)
Ca_2CuO_3[a]	0.3779	1.2239	0.3259
Sr_2CuO_3[b]	0.3912	1.2688	0.3485
Space group of all these phases is *Immm*			

[a] Teske and Müller-Buschbaum [3].
[b] Teske and Müller-Buschbaum [2].

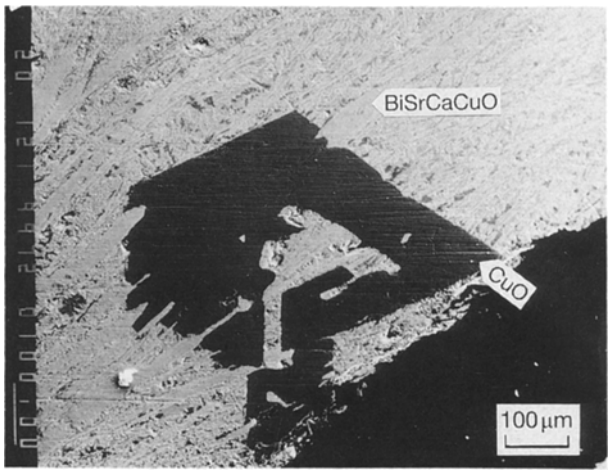

Figure 1 SEM photograph of a typical inclusion of a CuO crystal in the BiSrCaCuO bulk sample. The tabular crystals of BiSrCaCuO (in sections, see arrow) are smooth and light grey. Their composition is approximately $Bi_2Sr_{1.3}Ca_{1.2}Cu_{1.2}O_{6.7}$. The other phases filling space between them have not yet been identified because of the small size of the crystals. Sample Bi-9.

TABLE IV The single crystal data for CuO from sample Bi-12; precession camera, Nb-filtered MoK_α radiation, $\lambda = 0.07107$ nm

	a(nm)	*b*(nm)	*c*(nm)	β(°)
CuO (this work)	0.4688(8)	0.3417(5)	0.513(1)	99.57(6)
CuO[a]	0.46837(5)	0.34226(5)	0.51288(6)	99.54(1)
Space group	*C*2/*c*.			

[a] Åsbrink and Norby [15].

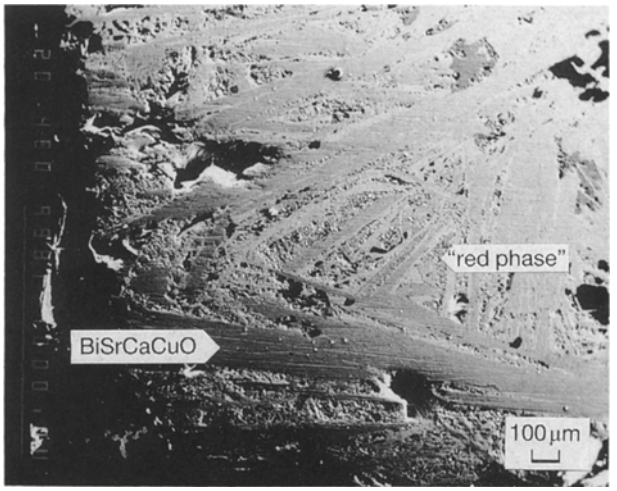

Figure 3 The SEM photograph of the polished section of sample Bi-6. The plate-like crystals of BiSrCaCuO are visible in section, like grey lamellae (see arrow). The space between crystals is filled by the "red phase" (black admixtures of Cu_2O in a light matrix of the phase).

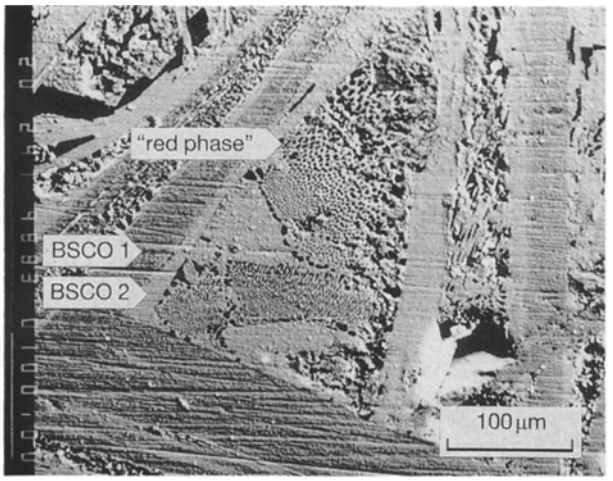

Figure 4 An enlarged part of the first image (triangular area right from the centre). The arrow labelled BSCO 1 shows the darker phase of composition $Bi_2Sr_{1.4}Ca_{1.3}Cu_{2.1}O_{7.6}$, the other one, labelled BSCO 2, shows the lighter phase of composition $Bi_2Sr_1Ca_{0.3}Cu_1O_{5.4}$. The inhomogeneity of the "red phase" is apparent.

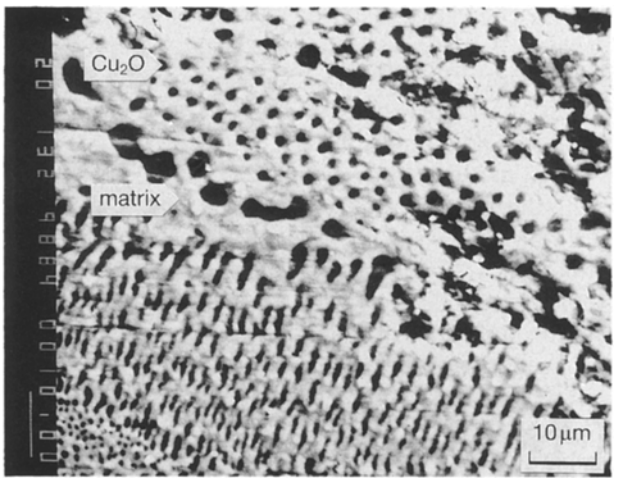

Figure 5 Detail of the internal structure of the "red phase". The different shape of admixtures of Cu_2O is given by the various angles of cross-section of their rod-like form. Some cross-sections of the Cu_2O rods have six-fold form (see, for example, upper left) suggesting its elongation along [1 1 1].

TABLE VI X-ray powder diffraction data of the mixed "red phase" from sample Bi-6; Gandolfi camera, Straumanis arrangement, CoK_α radiation (λ = 0.17902 nm), comparison with data for Cu_2O cuprite) and with calculated d-values for Bi_2SrCaO_5

"Red phase"			Cu_2O(JCPDS 5-667)			Bi_2SrCaO_5 (tentative match)	
2θ(°)	d_{obs}(nm)	I/I_0	d_{obs}(nm)	I/I_0	*hkl*	d_{calc}(nm)	*hkl*
22.8	0.453	2				0.4505	401
28.6	0.362	?				0.3652	402
30.3	0.342	2				0.3413	− 602
31.1	0.334	1				0.3394	− 312
34.5	0.302	10	0.30206	1	100		
35.1	0.297	5				0.2972	403
36.9	0.283	1d[a]				0.2850	204
38.9	0.269	1d[a]				0.2684	− 513
42.7	0.246	7	0.24645	10	111		
48.6	0.217	1				0.2167	021
49.6	0.213	3	0.21344	4	200		
50.5	0.210	3				0.2107	221
52.4	0.203	?				0.2030	514
54.0	0.1972	1d[a]				0.1970	− 10.0.4
55.3	0.1929	1d[a]				0.1935	− 316
61.5	0.1750	2d[a]	0.17430	< 1	211		
62.7	0.1720	2				0.1722	913
72.0	0.1523	1				0.1521	− 318
73.0	0.1505	2	0.15098	3	220		
81.4	0.1372	2				0.1371	12.2.0
88.6	0.1282	1	0.12868	2	311		
93.7	0.1227	1	0.12330	< 1	222		
102.0	0.1152	1					[b]
103.0	0.1144	1					[b]
104.8	0.130	1					[b]

[a] d = diffuse line.
[b] Indexing of lines with high 2θ was not unambiguous.

the electron microprobe analysis revealed that these admixtures contain Cu as the only metal present, whereas the light matrix is composed of another phase with only a small amount of Cu (see Table II). The chemical formula derived from this analysis is $Bi_4Sr_{1.45}Ca_{2.31}Cu_{0.37}O_{10.13}$. Roth *et al.* [1] report two phases in the SrO–CaO–$\frac{1}{2}Bi_2O_3$ ternary, of which Bi_2SrCaO_5 seems to be close to our phase, if we allow for some Sr replacement by Ca and the presence of Cu impurity. Since the size of cross-sections of the dark phase, as well as of areas of the matrix varied from 0.05 μm to 10 μm, the electron beam could not always be focused precisely enough to prevent exciting the other phase. The copper could be partially explained by this fact.

Attempts to obtain either a single crystal of the matrix phase or a fragment of an area with uniformly oriented admixtures were not successful. Several selected red fragments were mounted on a Gandolfi camera. The resulting powder data were compared with

the JCPDS PDF-1 files 1–40 [16]. The powder data, Table VI, appeared to represent a mixture of Cu_2O–cuprite [16] (not of CuO–tenorite, as we expected) and another phase. Since powder data for a possible candidate Bi_2SrCaO_5 were not yet available, we tried to index some of the remaining lines according to the lattice parameters given by Roth *et al.* [1] ($a = 2.187$, $b = 0.4385$, $c = 1.302$ nm, $\beta = 103.04°$, monoclinic, $C2/m$). Using the program CELREF of Appleman and Evans [17], other lines were indexed and the lattice parameters refined. The following values were obtained: $a = 2.161(15)$, $b = 0.440(1)$, $c = 1.297(6)$ nm, $\beta = 103.2°$. The resulting d_{calc} and *hkl* are given in Table VI. The match is not perfect, but probably acceptable. However, the lines with higher 2θ could not be indexed unambiguously.

The appearance of a material with this composition is not yet been explained, but it could be connected with high melting temperature (~ 1100 °C) and complicated treatment. Since some cross-sections of cuprite rods have six-fold form (see Fig. 5 upper left) we can suggest that they are oriented parallel with [111] of the cuprite cubic cell.

3.5. "Yellow phase"

This phase is contained in the samples heated to over 1040 °C, Bi-6, Bi-12 and Bi-22. The irregularly shaped crystals varied in colour from light to greenish yellow, were transparent, and optically isotropic. Since it was difficult to distinguish them on the SEM images of the polished sections, the microprobe analyses were performed on separated fragments. The results of the analyses (Table II) showed that this phase contains Bi, Ca, Sr and Al (from the crucible), but practically no Cu. The formula derived from the analysis is $Bi_{1.22}Sr_{1.95}Ca_{1.02}Cu_{0.10}Al_3O_{9.4}$ for Bi-6, $Bi_{1.29}Sr_{1.53}Ca_{0.99}Cu_{0.08}Al_3O_{9.03}$ for Bi-12 and $Bi_{1.05}Sr_{1.94}Ca_{0.86}Cu_{0.18}Al_3O_{9.05}$ for Bi-22. The ideal formula supposing trivalent Bi and omitting Cu is $BiSr_2CaAl_3O_9$.

Single crystals for X-ray investigation were separated from samples Bi-6 and Bi-22. The *hhl* and *Okl* precession photographs, [100], [110] cone-axis photographs, and [100], [110] and [111] front reflection Laüe photographs revealed a cubic symmetry. The lattice parameter, from precession photograph is $a = 2.486(6)$ nm for Bi-6 and $a = 2.496(8)$ nm for Bi-22. Systematic extinctions (*OOl*: $l = 2n$; *Okl*: $k + l = 4n$, $k = 2n$, $l = 2n$; *hhl*: $h + l = 2n$) allow possible space groups $Fm\bar{3}m$, $F\bar{4}3m$, $F432$, $Fm\bar{3}$ and $F23$.

Powder data from the same samples were obtained on a Gandolfi camera. Theoretical *d*-values of several of the most intense diffraction spots on precession photographs were calculated, corresponding lines

TABLE VII X-Ray powder diffraction data of the "yellow phase"; Gandolfi camera, Straumanis arrangement, CoK_α radiation ($\lambda = 0.17902$ nm)

From Sample Bi-6				From sample Bi-22				
2θ(°)	d_{obs}(nm)	I/I_0	d_{calc}(nm)	2θ(°)	d_{obs}(nm)	I/I_0	d_{calc}(nm)	*hkl*
28.1	0.368	1	0.3732	27.9	0.371	2	0.3737	622
				29.1	0.356	?	0.3578	444
30.2	0.344	2	0.3466	30.0	0.346	2	0.3471	551
32.3	0.322	9	0.3223	32.3	0.322	9	0.3227	553
				33.5	0.311	1	0.3099	800
34.6	0.301	8	0.3002	34.6	0.301	8	0.3006	446
35.6	0.293	10	0.2917	35.7	0.292	10	0.2921	660
36.5	0.286	2	0.2858					555
38.5	0.271	2	0.2717	38.8	0.269	2	0.2721	911
39.6	0.264	1	0.2638	39.7	0.264	1	0.2643	664
49.1	0.215	2	0.2154	48.9	0.216	2	0.2158	882
50.8	0.209	2	0.2092	50.5	0.210	2	0.2095	10.6.2.
52.8	0.201	1d[a]	0.2008					12.2.2.
55.0	0.1939	4	0.1939	55.1	0.1935	4	0.1941	991
56.3	0.1897	3	0.1893	56.4	0.1894	3	0.1896	11.7.1.
57.9	0.1849	3	0.1850	57.7	0.1855	3	0.1853	13.3.1.
				59.1	0.1815	1	0.1813	13.3.3.
61.3	0.1756	5	0.1750	61.3	0.1756	5	0.1753	10.10.0.
61.9	0.174	?	0.1737					11.9.1.
64.3	0.1682	2d[a]	0.1684	64.1	0.1687	1d[a]	0.1687	14.4.2.
65.9	0.1646	1	0.1643	66.0	0.1643	1	0.1645	15.1.1.
68.6	0.1588	2	0.1588	68.4	0.1592	2	0.1590	15.3.3.
69.5	0.1570	2	0.1570					12.10.2.
70.1	0.1559	1	0.1562	69.8	0.1564	1	0.1565	13.9.1.
73.1	0.1503	1d[a]	0.1501					16.4.0.
75.7	0.1459	1	0.1459					12.12.0.
80.7	0.1382	2	0.1384	81.0	0.1378	1d[a]	0.1377	16.8.2.
95.0	0.1214	1	0.1214	95.5	0.1209	1		[c]
				117.6	0.1046	2		[c]
				135.6[b]	0.1005	1d[a]		[c]
				151.5[b]	0.0922	1d[a]		[c]

[a] d = diffuse line.
[b] α_1 line ($\lambda = 0.17889$ nm).
[c] Indexing of lines with high 2θ was not unambiguous.

were found in the powder data and respective indices allotted. The remaining lines were indexed and lattice parameter refined by the program of Appleman and Evans [17]. The resulting lattice parameter is $a = 2.4754(9)$ nm for Bi-6 and $a = 2.479(1)$ nm for Bi-22. The program of Burnham [18] was also tried with the results $a = 2.4760(8)$ nm for Bi-9 and $a = 2.4801(8)$ nm for Bi-22. These values are shifted with respect of those from the precession camera. It must be mentioned, that the lines with high diffraction angle were weak and diffuse, so that the correction due to the Straumanis arrangement could not be done with sufficient reliability.

The indexed powder data from both samples are given in the Table VII. However, since some lines of higher 2θ could not be indexed unambiguously, their indices are omitted. A check of the JCPDS PDF-1 file series 1–40 [16] yielded no satisfactory matches. The crystal structure determination is now under way.

3.6. Other phases

There are also other colourless crystals in many samples. The preliminary electron microprobe study revealed at least four different compositions for the same crystal morphology. Further study of these crystals is now under way. Unfortunately, crystals of other, additional phases were so small that X-ray studies and microprobe analysis (because of problems with beam focusing) were not possible.

4. Conclusions

In most of the studied samples (except Bi-26) the 2212 and/or 2201 phases were identified by means of X-ray diffraction (powder or single crystal) and of electron microprobe analysis. CuO crystals appear in most samples on the surface or embedded in the bulk mass. Ca_2CuO_3 appeared in one sample (Bi-26) as its highly prevalent phase, whereas crystals of other phases were too small to be identified. The "yellow phase" is a product of reaction of alumina crucibles with its contents and appeared in three samples heated to over 1040 °C. The admixtures of Cu_2O and $Bi_4Sr_{1.45}Ca_{2.31}Cu_{0.37}O_{10.13}$ in the "red phase" is probably a result of complicated treatments. Instead of forming a single phase, Cu precipitates as Cu_2O and other elements form the matrix phase.

Acknowledgements

We thank Dr I. Velická for her aid with the optical studies, Ms D. Uherová for the copying of photographs and Ms M. Zatočilová for careful preparation of polished sections.

References

1. R. S. ROTH, C. J. RAWN, B. P. BURTON and F. BEECH, *Abstr. Am. Crystallogr. Assoc. ser.* 2, **17** (1989) 41.
2. CHR. L. TESKE and H. K. MÜLLER-BUSCHBAUM, *Z. Anorg. Allg. Chem.* **371** (1970) 325.
3. *Idem. ibid.* **379** (1970) 234.
4. *Idem. ibid.* **370** (1969) 134.
5. *Idem. ibid.* **379** (1970) 113.
6. P. CONFLANT, J.-C. BOIVIN and D. THOMAS, *J. Solid State Chem.* **18** (1976) 133.
7. R. GUILLERMO, P. CONFLANT, J.-C. BOIVIN and D. THOMAS, *Rev. Chim. Miner.* **15** (1978) 153.
8. N. M. HWANG, R. S. ROTH and C. J. RAWN, *J. Amer. Ceram. Soc.* **73** (1990) 2531.
9. B. HONG, J. HAHN and T. O. MASON, *ibid.* **73** (1990) 1965.
10. S. DURČOK, M. NEVŘIVA, L. MATĚJKOVÁ, J. HEJTMÁNEK, P. VASEK, M. ŠIMEČKOVÁ, E. POLLERT and A. TŘÍSKA, *Czech. J. Phys.* **B39** (1989) 113.
11. G. GANDOLFI, *Mineral. Petrogr. Acta* **10** (1964) 149.
12. *Idem., ibid.* **13** (1967) 67.
13. Y. K. HUANG, K. KADOWAKI, M. J. V. MENKEN, J. N. LI, K. BAKKER, A. A. MENOVSKY, J. J. M. FRANSE, G. F. BASTIN, H. J. M. HEIJLIGERS, H. BARTEN, J. VAN DEN BERG, R. A. ZACHER and H. W. ZANDBERGEN, *Physica C* **152** (1988) 431.
14. Y. GAO, P. LEE, P.COPPENS, M. A. SUBRAMANIAN, A. W. SLEIGHT, *Science* **241** (1988) 954.
15. S. ÅSBRINK and L. J. NORBY, *Acta crystallogr.* **B26** (1970) 8.
16. JCPDS PDF-1 Powder Diffraction File Series 1–40 (JCPDS-ICDD, Swarthmore, 1990).
17. D. E. APPLEMAN and H. T. EVANS Jr, in "U.S. Geological Survey Computer Contribution 20, U.S. National Information Service Document PB2-16188 (U.S. National Information Service, Washington, DC. 1973). (Modified by P. C. Burns and L. Trembath.)
18. C. W. BURNHAM, *Carnegie Institution Year Book* **61** (1962) 132.

Received 26 February
and accepted 10 December 1992